

Role of interfacial oxide-related defects in the red-light emission in porous silicon

S. M. Prokes and O. J. Glembocki

Naval Research Laboratory, Washington, D.C. 20375

(Received 20 October 1993)

Intense laser irradiation has been used to anneal porous silicon. *In situ* Raman spectroscopy and photoluminescence (PL) spectroscopies have been used as probes of the silicon particle sizes and temperatures, and the resulting light emission of porous silicon. Once annealed, the PL of porous silicon while at 830 °C exhibited no PL energy shift from its 300-K position. Since the gap of silicon redshifts by 0.29 eV at 830 °C, this red PL cannot be the property of the Si particles. A model involving the presence of nonbridging oxygen hole centers has been suggested to account for this PL.

Reports of visible photoluminescence (PL) in porous silicon¹ have led to questions concerning the luminescence mechanism. Although significant data exists in porous silicon, no single model has been able to consistently explain all the results. One mechanism which has been suggested¹ involves carrier recombination within a quantum size silicon particle. Competing models include siloxene,² surface polysilanes,³ SiH₂,⁴ and Si band-tail states⁵ as the source of the luminescence.

In this work, the effect of laser heating on the Raman and PL spectra will be examined, along with effects on the particle size distributions and the PL peak energy. The above results will show that the PL cannot be a property of the silicon microcrystallites or silicon band-tail states. A model will be presented with supporting evidence suggesting the source of the PL is a localized surface defect, very similar to a nonbridging oxygen hole center (NBOHC).

Porous silicon samples were prepared by electrochemical etching of 0.1 and 1 Ω cm *p*-type Si(100) wafers at a current density of 30 mA/cm² for 2–30 min in a 25% hydrofluoric acid (HF)–ethanol solution. Several samples were also open-circuit etched for 30 min in a 25%–ethanol solution. The samples were examined by optical microscopy, Raman spectroscopy (RS), and photoluminescence. Two optical spectrometers and a single laser (488-nm line of the Ar⁺ laser) were used to obtain the RS and PL. The laser that was used for the optical measurements was also used to anneal the samples. In this manner, it was possible to obtain both the vibrational and light emission properties of the porous silicon during laser annealing and subsequent cooling. This is extremely important, since, as will be shown, Raman spectroscopy can be used to accurately determine the temperature of the porous silicon while heating, as well as the average particle size, which can then be used to address the effect of particle size and heating on the PL. An EG&G model 1453A spectrometer with an optical multichannel analyzer was used for detection of the PL, and a SPEX 1877 triple spectrometer equipped with an EG&G model 1420 optical multichannel analyzer using a nominal back-scattering geometry was used in the case of Raman spectroscopy. The irradiated 100-μm spot was also observed

using a video system, to ascertain that the laser spot remained on the same region of the sample upon changing of laser powers.

A typical PL scan of a 1-Ω cm sample etched at 30 mA/cm² for 30 min in a 25% HF–ethanol solution is shown in Fig. 1(a). The as-made sample refers to a fresh sample, using a very low laser power (10 mW), where no heating of the sample is apparent (300 K). The second PL spectrum is obtained from an identical spatial region of the sample, but laser heated in the ambient to a temperature of 1100 K. The sample was annealed for 2 min, and then allowed to cool to room temperature. The local temperature (within the illuminated spot) was determined by RS, as will be discussed later. First note that the initial PL is quite weak, and in the 1.5-eV range. After laser heating, the PL blueshifts significantly, to 1.72 eV, and increases in intensity by a factor of 24. The PL energy remains at the same value with any further laser heating.

The Raman spectrum for the preannealed state of the sample is shown in Fig. 1(b). The Raman spectrum in this figure was fit using two Lorentzians (shown in solid line), corresponding to an amorphous silicon⁶ structure near 480 cm⁻¹ and a sharper line at 501 cm⁻¹. The 501-cm⁻¹ peak is associated with a particle size distribution in porous silicon, as has been discussed in previous works.^{7–10} In fact, Kanemitsu *et al.*¹⁰ compared experimentally determined particle sizes of various porous silicon samples using transmission electron microscopy, optical absorption, and RS, to those obtained by modeling spheres of diameter *L*. They found very good agreement between the Raman spectra from experiment and from the modeled spheres. Using the results of Kanemitsu *et al.*,¹⁰ the average particle size of the as-made porous silicon sample shown in Fig. 1(b) corresponds to 2.1 nm (diameter). In our experiment, the Raman line sharpens significantly and blueshifts to 0.5 cm⁻¹ below that of bulk silicon with the high power laser heating [see Fig. 1(b)]. This corresponds to an average particle diameter in excess of 20 nm,⁷ suggesting that laser heating has resulted in significant particle coarsening. In addition, the volume of amorphous silicon has decreased by 95%, a result obtained directly from the area of the amorphous Raman peak before and after laser annealing. Since amorphous

silicon easily crystallizes at temperatures as low as 450°C,¹¹ it is likely that an amorphous silicon layer surrounding the x -Si particles crystallizes with the heat treatment, resulting in larger x -Si particles. This is quite reasonable, since, as will be shown later, this high laser power leads to heating of the Si particles to temperatures of 1100 K, which would certainly allow the crystallization process to proceed rapidly (88 nm/sec).¹¹ Also, particle coarsening has been reported for higher temperature anneals (above 450°C) in previous works,^{12,13} which could not occur by a general Si diffusion, since the structure is quite porous and contains various hydrides and/or oxides surrounding the particles.¹⁴

Although the particle size increases from 2.1 to more than 20 nm, the PL blueshifts by 0.22 eV, exactly the opposite of what would be expected if the PL was the result of band-to-band recombination in quantum-confined particles. It should also be noted that PL from 20-nm quantum-confined Si spheres would occur near 1.15 eV rather than the observed 1.72 eV.

When the same sample (different spot) was subjected to open-circuit etching in 25% HF-ethanol for 30 min, a 3-nm particle size distribution was obtained from Raman spectroscopy. The PL blueshifted to 1.82 eV and increased in intensity, and the relative volume of the amor-

phous silicon Raman line decreased. After laser annealing to 1100 K, the PL intensity further increased, the PL redshifted to 1.72 eV, the particle size increased to greater than 20 nm, and the relative volume of amorphous silicon further decreased. Thus, pore "widening" led to a blueshift in the PL by 0.32 eV and an intensity increase, although the average particle size was larger in the blueshifted sample.

From these results, it appears that the PL energy does not correlate with the particle size. It should also be mentioned that PL energy in the range of 1.7 eV has been obtained in various porous silicon samples after the laser heating experiments and after furnace oxidation,¹⁵ regardless of initial etching conditions or substrate doping. It cannot be shifted by any further oxidation¹⁵ nor by any further laser heating (this experiment).

RS was also used to determine the temperature of the silicon crystallites. Figure 2(a) shows plots of the Raman spectra originating from the Si crystallites as a function of laser heating. The room-temperature Raman line is from the sample shown in Fig. 1(b), which exhibits the usual high PL intensity at 1.72 eV. The Raman line broadens and significantly redshifts as a function of increased laser power. This is an indication of increased heating within the particles, which are efficient at absorbing the laser power, but cannot shed heat efficiently, be-

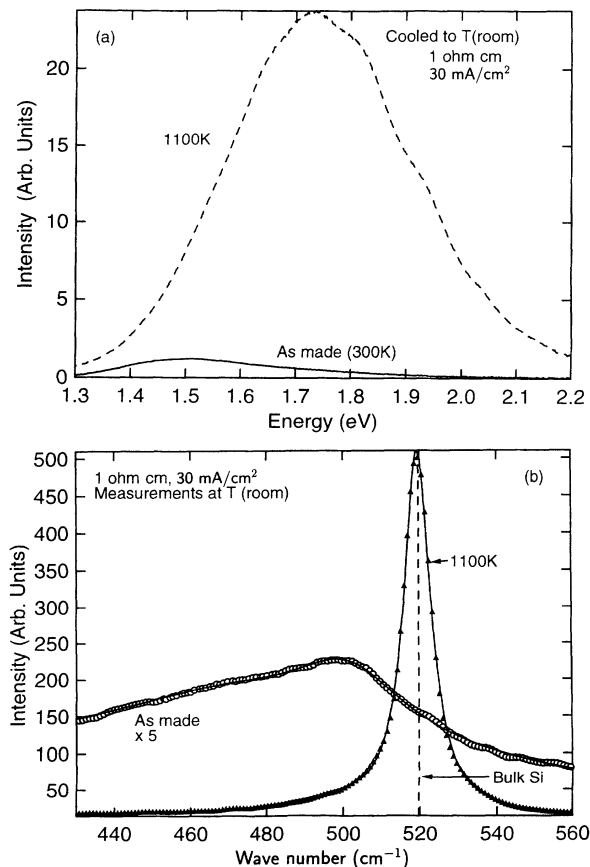


FIG. 1. (a) PL lines of as-made 1- Ω cm porous silicon sample and for laser-annealed sample to a temperature of 1100 K and (b) Raman spectra of above sample. All measurements were performed at room temperature.

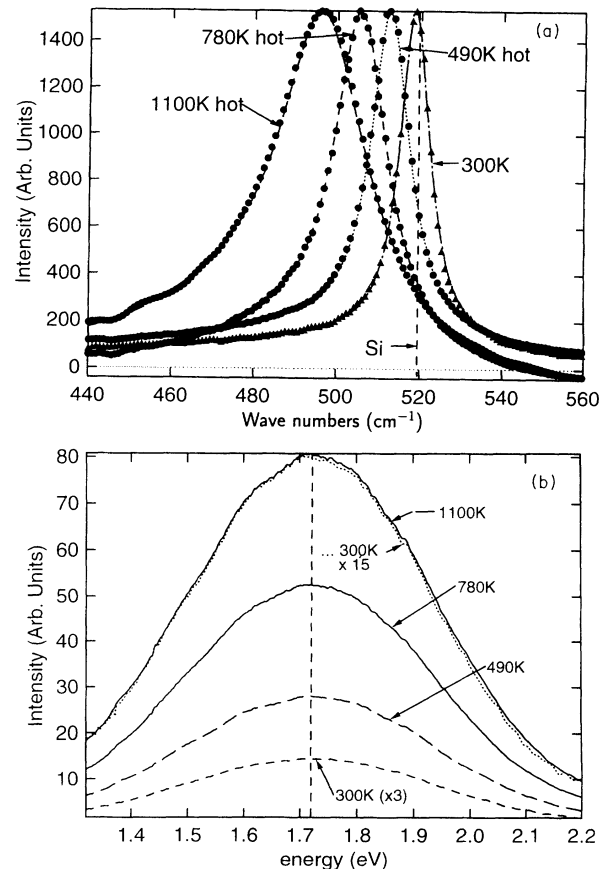


FIG. 2. (a) Shift of the Raman spectra of the sample in Fig. 1 with increasing laser heating and (b) PL lines of the above sample. Measurements were performed at the temperatures indicated.

ing relatively isolated from a heat sink. The Raman redshift and broadening is directly related to the resulting Si particle temperature,¹⁶ as shown in Fig. 2(a). In order to confirm this result, Stokes–anti-Stokes measurements were performed on the same sample for several laser powers, with the resulting temperatures being in good agreement with those obtained above.

Thus, both the Raman signal (in effect, a Si particle temperature gauge) and the PL during the heating and upon cooling to room temperature could be monitored, as shown in Figs. 2(a) and 2(b). Figure 2(b) is a plot of the PL at various temperatures, and plot 2(a) shows the corresponding Raman signals from which the temperature was determined. It is important to note that there is no change in the PL line shape or its peak position.

In order to ensure that the whole porous silicon sample was heated as a function of depth, a thinner porous silicon sample was also prepared under identical etching conditions, which also exhibited a Si substrate Raman line. In this case, the porous silicon Raman lines shifted with laser heating, while the Si substrate line did not. Although the resulting heating of the porous silicon particles was less (due to a better heat sink), the behavior of the PL was identical to that shown in Fig. 3. This indicates that the PL originates from the heated porous silicon layer.

The lack of a PL energy shift or line-shape change with increasing temperatures is very revealing, because under these conditions, the Si band gap decreases according to $E_G(T) = E_G(0) - AT^2/(T+B)$,¹⁷ where T is the temperature, and A and B are constants. The Si gap, along with the PL energy of the porous silicon, is shown in Fig. 3 for the temperature range of interest. Clearly, the PL does not track in any way with the expected shrinking of the Si gap. This leads to the inevitable conclusion that the PL reported in the 1.72-eV range from porous silicon cannot be due to recombination within the Si crystallites exhibiting quantum confinement, as proposed by Canham.¹ This result also puts in question the idea that the PL originates from silicon band-tail states.⁵ If the band-tail states are silicon related, then their position would be sensitive to the annealing temperature and a PL originating from them would be sensitive to temperature.¹⁸ It is

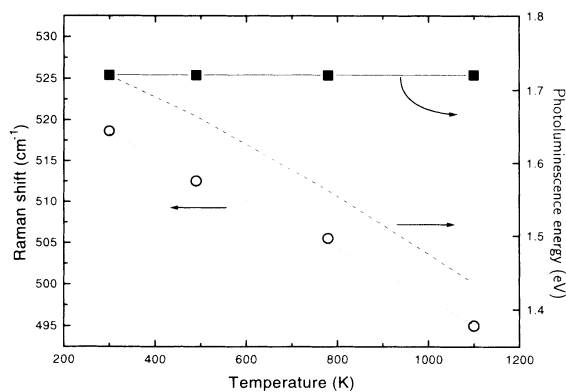


FIG. 3. Shift of (a) Raman spectra with temperature (\circ), (b) shift of the Si gap with temperature (— — —), and (c) PL energy of heated porous silicon as a function of temperature (\blacksquare).

much more likely that the PL originates from a surface-related localized defect, such as the NBOHC,¹⁹ as suggested previously.¹⁵ These centers have been reported in silica optical fibers and they luminesce in the red (600–670 nm) at room temperature, with a peak width (full width at half maximum) around 0.35 eV.^{20–22} Three different NBOHC types have been identified,²² which vary in PL energy and quantum efficiencies. The first type of NBOHC is Si-O^- , which exhibits a lower energy PL (more red) with lower quantum efficiencies, and does not appreciably shift with heat treatments.²² The second type of NBOHC is stabilized with a hydrogen bond, such as $\text{Si-O}^- \cdots \text{H-Si}$. This type of defect was seen in silica containing high concentrations of hydroxyls or hydrides, and exists only at temperatures below 350°C. It has been shown to blueshift with increasing hydrogen content, along with an increase in quantum efficiency.^{21–23} The reverse is also true, in that the PL redshifts and drops in intensity with hydrogen loss.²² The least understood NBOHC is likely caused by the strain of bonding at an interface between two materials of different bond lengths, density, or structure, and it has been reported after the drawing of oxide clad fibers and after high-temperature annealing.²³ Finally, the NBOHC's which are stable at higher temperatures (as high as 800°C) do not show any PL line shift or shape change during heating to high temperature compared to PL at room temperature.²²

Now let us examine some results from porous silicon. The room-temperature PL has been reported in the red,¹ with a PL peak width in the 0.3-eV range. The PL has been reported to increase and blueshift with HF open-circuit etching,¹ which can also increase the hydride content.²⁴ Also, the PL in porous silicon has been reported to redshift along with a loss of hydrogen, both by heating³ and by room-temperature UV irradiation.²⁵ This behavior is also exhibited by the second type of NBOHC. Furthermore, since the NBOHC's are localized defects, the PL time decay is nonexponential,¹⁹ as has been reported for porous silicon.²⁶ The most convincing evidence, however, is from the temperature behavior of the PL. As reported in this paper, porous silicon heated to 830°C and at room temperature exhibits no PL shift or shape change, exactly the same behavior as reported for the high-temperature NBOHC's.²² Also, porous silicon samples which remained in the atmosphere for several months always exhibit a much more intense PL, and generally blueshift to some extent (this experiment). *Identical* behavior has been reported for NBOHC, which pick up OH groups from the atmosphere, leading to a PL increase and blueshift, due to stabilization of NBOHC's by hydrogen.²³

Let us now consider a model for the PL in porous silicon. As discussed earlier, the porous silicon structure consists of a crystalline silicon core, surrounded by some amount of amorphous silicon, which may contain hydrides and possibly some oxygen. SiO_2 surrounds this structure,¹⁴ especially in samples which have had contact with the atmosphere or which were heated or oxidized. Experimentally, the PL intensity increases with decreasing amorphous silicon volume (V_a), that is, $I \propto 1/V_a$, directly obtained from a comparison of the Raman and

PL results. For example, the ratio of V_α of the as-made sample to the V_α of the heated and cooled sample shown in Fig. 1(b) is 26. From the PL in Fig. 1(a), $I(\text{heated})/I(\text{as made})=24$, very close to the prediction obtained from inverse volumes of amorphous silicon. This relation has been tested on various other samples, with equal success. Thus, as the volume of the amorphous silicon "buffer" layer between the oxide and the crystalline silicon nanostructures decreases, the PL intensity increases. In the case of no "buffer" layer, a significant strain would exist at the abrupt x-Si-oxide interface, due to the much more open structure of the oxide. In some way, this is analogous to epitaxy between two crystalline materials of differing lattice parameters. Since this interface is quite abrupt, defects such as Si dangling bonds or broken Si-O-Si bonds will be created. If, however, the interface now becomes more diffuse, the strain will be distributed over a larger volume, resulting in a reduced number of defects at the Si-oxide interface. Here, the broadening of the interface is achieved by the amorphous silicon buffer layer, which is a continuous random network and similar in lattice parameter to x-Si. One can relate the number of defects at that interface to the strain and buffer layer volume as follows: $N \propto \epsilon/V_\alpha$, where N is the number of defects per area and ϵ is the strain if a sharp interface existed. If the defects in question are the NBOHC, then the PL intensity would be expected to scale with the number

of defects at the interface, and thus, $I_{\text{PL}} \propto N \propto 1/V_\alpha$, as is observed experimentally. It should be mentioned that the above $1/V_\alpha$ dependence is only approximate, since the oxygen content at the interface, the curvature of the interface, particular hydrogen bonding, and the relative ratios of the three NBOHC's should affect the intensity in various samples.

In conclusion, RS and PL results have been presented. The results indicate that laser heating can raise the Si nanostructures to temperatures as high as 830°C, which leads to the crystallization of amorphous silicon. This in turn leads to a particle size increase from 2 to over 20 nm, accompanied by a large PL intensity increase. Furthermore, the PL of porous silicon obtained while at 830°C resulted in no energy shifts or shape change compared to room temperature. Since the gap of silicon redshifts by 0.29 eV at this temperature, this red PL from porous silicon cannot be caused by quantum confinement of the Si particles, nor by band-tail states. A model involving the presence of NBOHC's has been suggested to account for this PL, which appear to behave very similarly to porous silicon.

The authors would like to thank G. Brozak, B. V. Shannabrook, W. E. Carlos, D. Griscom, R. C. Cammarata, and M. Peckerar for helpful discussions, and D. King for help in sample preparation.

- ¹L. E. Canham, Appl. Phys. Lett. **57**, 1046 (1990).
- ²M. S. Brandt, H. D. Fuchs, M. Stutzmann, J. Weber, and M. Cardona, Solid State Commun. **81**, 307 (1992).
- ³S. M. Prokes, O. J. Glebocki, V. M. Bermudez, R. Kaplan, L. E. Friedersdorf, and P. C. Searson, Phys. Rev. B **45**, 13 788 (1992).
- ⁴C. Tsai, K. H. Li, D. S. Kinosky, R. Z. Qian, T. C. Hsu, J. T. Irby, S. K. Banerjee, B. K. Hance, and J. M. White, Appl. Phys. Lett. **60**, 1700 (1992).
- ⁵F. Koch, V. Petrova-Koch, T. Muschik, A. Nikolov, and V. Gavrilenko, in *Microcrystalline Semiconductors: Materials Science and Devices*, edited by P. M. Fauchet *et al.*, MRS Symposia Proceedings No. 283 (Materials Research Society, Pittsburgh, 1993), p. 197.
- ⁶J. M. Perez, J. Villalobos, P. McNeill, J. Prasad, R. Cheek, J. Kelber, J. P. Estrera, P. D. Stevens, and R. Glosser, Appl. Phys. Lett. **61**, 563 (1992).
- ⁷I. H. Campbell and P. M. Fauchet, Solid State Commun. **58**, 739 (1984).
- ⁸R. Tsu, H. Shen, and M. Dutta, Appl. Phys. Lett. **60**, 112 (1992).
- ⁹Shifeng Sui, Patrick P. Leong, Irving P. Herman, Gregg S. Higgashi, and Henryk Temkin, Appl. Phys. Lett. **60**, 2086 (1992).
- ¹⁰Y. Kanemitsu, H. Uto, Y. Masumoto, T. Matsumoto, T. Futagi, and H. Mimura, Phys. Rev. B **48**, 2827 (1993).
- ¹¹L. Csepregi, E. F. Kennedy, T. J. Gallagher, J. W. Mayer, and T. W. Sigmon, J. Appl. Phys. **48**, 4234 (1978).
- ¹²G. Bomchil, R. Herino, and K. Barla, in *Proceedings of the European MRS Meeting, Strasbourg*, edited by V. T. Nguyen and A. G. Cullis (Elsevier North-Holland, Amsterdam, 1985), Vol. 4, p. 463.
- ¹³T. Ito, T. Yasumatsu, H. Watabi, and A. Hiraki, Jpn. J. Appl. Phys. **29**, L201 (1990).
- ¹⁴A. G. Cullis and L. T. Canham, Nature **353**, 335 (1991).
- ¹⁵S. M. Prokes, Appl. Phys. Lett. **62**, 3244 (1993).
- ¹⁶H. Tang and I. P. Herman, Phys. Rev. B **43**, 2299 (1991).
- ¹⁷J. W. Mayer and S. S. Lau, *Electronic Materials Science: For Integrated Circuits in Si and GaAs* (Macmillan, New York, 1990), p. 76.
- ¹⁸R. Fischer, in *Topics in Applied Physics: Amorphous Semiconductors*, edited by M. H. Brodsky (Springer-Verlag, Berlin, 1979), p. 159.
- ¹⁹D. L. Griscom, J. Ceram. Soc. Jpn. **99**, 923 (1991).
- ²⁰L. N. Skuja and A. R. Silin, Phys. Status Solidi A **56**, K11 (1979).
- ²¹K. Nagasawa, Y. Ohki, and Y. Hama, Jpn. J. Appl. Phys. **26**, L1009 (1987).
- ²²S. Munekuni, T. Yamanaka, Y. Shimogaichi, R. Tohmon, Y. Ohki, K. Nagasawa, and Y. Hama, J. Appl. Phys. **68**, 1212 (1990).
- ²³K. Nagasawa, Y. Hoshi, Y. Ohki, and K. Yahagi, Jpn. J. Appl. Phys. **25**, 464 (1986).
- ²⁴S. M. Prokes, W. E. Carlos, and V. M. Bermudez, Appl. Phys. Lett. **61**, 1447 (1992).
- ²⁵R. T. Collins, M. A. Tischler, and J. H. Stathis, Appl. Phys. Lett. **61**, 1649 (1992).
- ²⁶Y. H. Xie, W. L. Wilson, F. M. Ross, J. A. Muha, E. A. Fitzgerald, J. M. Macauley, and T. D. Harris, J. Appl. Phys. **71**, 2403 (1992).